Beeswax Material: Non-Conventional Solid Fuel for Hybrid Rocket Motors

A. El-S. Makled*

Space Technology Centre, Cairo, Egypt

Abstract:

Traditional solid fuel for Hybrid Rocket Motor (HRM) is characterized as a low regression rate, aiming to develop a new generation of solid fuel material that combines at the same time good ballistic properties, easy manufacture, safe exhaust emission and low cost. Beeswax as bio-derived hydrocarbon fuel has been evaluated to be used as solid fuel in HRM. Firing tests are carried out at the average pre-chamber pressure of 2.90 bar, the oxidizer mass flow rate of 9.34 g/s and the regression rate of 1.5 mm/s at combustion efficiency reaches 60.3 %. Beeswax as pure solid fuel grain at 7 mm active channel port with 100 mm length is tested with gaseous oxygen (gO_2) as oxidizer and it showed a regression rate at least three times as high as traditional hybrid propellant, such as Polymethyl methacrylate (PMMA) and Polyethylene (PE)/gO2. This provides a promise for high performance parameters with a special regression rate to overcome the main drawbacks of traditional hybrid propellant. Experimental evaluation parameters (regression rate, fuel mass flow rate and combustion efficiency) are carried out for beeswax/gO_2. Combustion shows fairly successful results for lab scale testing but it needs further enhancement, especially in combustion efficiency and theoretical studies for combustion efficiency.

Keywords:

hybrid rocket motor, solid fuel grain, beeswax, combustion, ignition system

1. Introduction

Recent trends in Propulsion system conceptual design are directed to adopt available and emerging technologies to attain high degree of performance, reliability and safety with low cost. Hybrid propulsion system (HPS) is powered by a combination of two old propulsion types, solid and liquid propulsion systems. It is still requiring more investigations for a better performance [1, 2].

---

* *Corresponding author: Space Technology Centre, Egyptian Army, Kobry Al-Kobbah, Cairo, Egypt. Phone: +20 10 378 48 89, fax: +20 2 263 4 26 98, E-mail: ahmak2007@yahoo.com*

The typical classical HPS configuration utilizes a solid fuel grain with a gas or liquid oxidizer. Reverse HPS is utilizing a solid oxidizer grain and liquid or gas fuel, which is not widely used. A schematic diagram of a typical HPS is shown in Fig. 1. Classical HPS consists of a solid fuel with gas or liquid oxidizer stored in different states. It has a high-performance parameters and specifications as high specific impulse, throttleable, restartable, storable, design flexibility and safety. These specifications present a favourable alternative similar to solid or liquid propulsion systems for many applications.

Several publications during the last 10 years show the curiosity of hybrid propulsion system in various field of researches, as launch vehicle, space propulsion, sounding rockets and educational pursues [1, 3, 4]. However, HPS has historically been inhibited by slow-burning solid fuels; it can be solved through the use of wax-based fuels as paraffin or beeswax.

In recent years, the interest on HPS technology using waxy solid fuel has grown up in some of the colleges and universities as Alabama, Arizona, Arkansas, US air force academy, Pennsylvania, Surrey, Stanford and Utah. The history of HPS dates back to the early years in 1933, USSR, the first flight system is GIRD-09 rocket. It is developed by Sergei Korolev and Mikhail Tikhonravov, it used a gelled gasoline as fuel and oxygen as oxidizer to generate 0.5 kN thrust that reached to ≈ 0.4 km altitude [4].
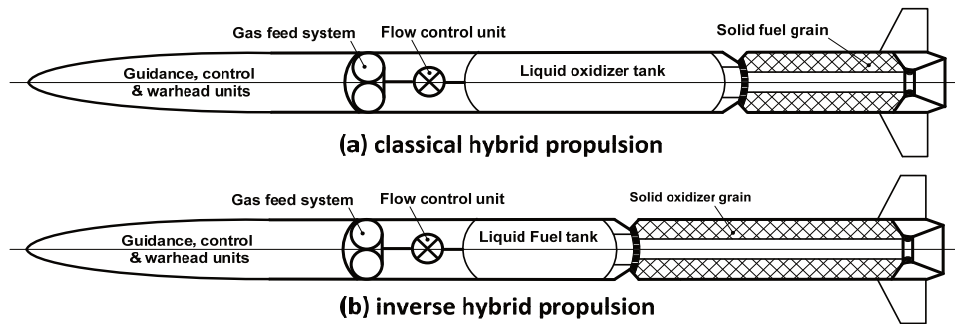

Fig. 1 Schematic diagram of a typical hybrid propulsion system

2. Experimental Work

2.1. Objectives

The direct goal of the firing test is to realize the proper investigation and analysis for ignition and combustion of beeswax / gO_2. Moreover, the objective is extended to examine the low cost and green ignition system (200 V NiCr coil igniter) and finally, to formulate and evaluate the regression rate, fuel mass flow rate and combustion efficiency of beeswax / gO_2 HRM.

2.2. Laboratory Test Facility

The beeswax / gO_2 HRM test facility comprises two parts, HRM test stand zone and control with recording room as shown in Fig. 2. The HRM exhaust gases are directed to open area and the test stand is separated from the control room by concrete wall with special glass observation window. The HPS comprises two main parts; small scale HRM that uses beeswax solid fuel charge and feed system for gO_2 as an oxidizer as shown in Fig. 3. The initiation of combustion is secured by the use of ignition system that employs

NiCr coil; Fig. 4 illustrates beeswax / gO_2 HRM firing test phases (ignition, steady state combustion and shout-off).

The small scale HRM is easily connected to gO_2 gas supply system through a 2.5 m high pressure Teflon hose with the external diameter of 6 mm for easy handling. The front flange has a 5 mm diameter centre hole that acts as gO_2 injector coaxial with the active port of fuel grain bore. The combustion takes place inside the fuel grain active channel port. gO_2 oxidizer is supplied to the HRM grain port for a firing time of 5.0 s.
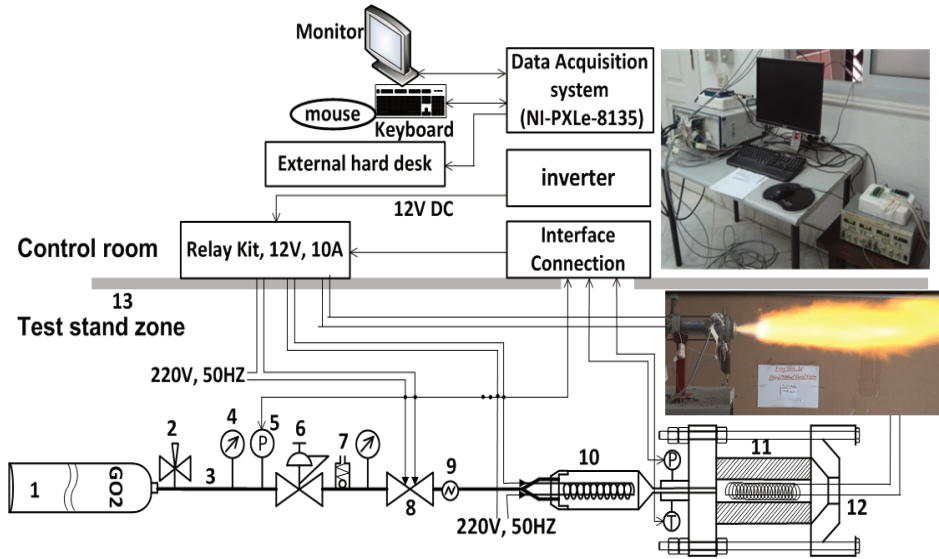
1 – gO_2 oxidizer tank, 2 – needle valve, 3 – pipe lines (6 mm diameter copper and Teflon), 4 – pressure gauge, 5 – pressure transducer, 6 – pressure regulator, 7 – safety regulator, 8 – on- off valve (solenoid valve), 9 – rotameter, 10 – heat exchanger, 11 – HRM, 12 – ignition system, 13 – temperature thermocouple.

Fig. 2 Schematic test facility, main components
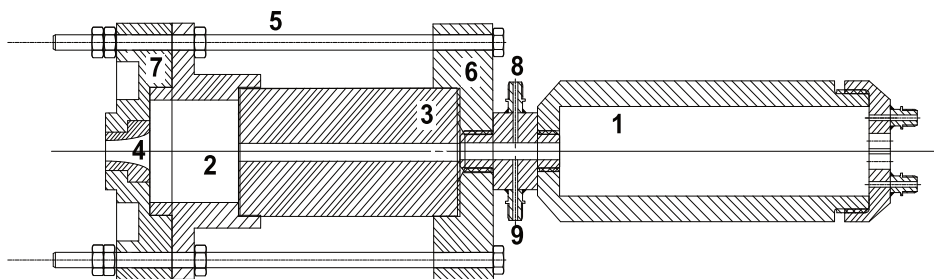
1 – heat exchanger, 2 – post-combustion chamber, 3 – fuel grain solid, 4 – graphite nozzle, 5 – screw bolts with nuts, 6 – front flange, 7 – rear flange, 8 – thermocouple connection, 9 – pressure transducer connection.

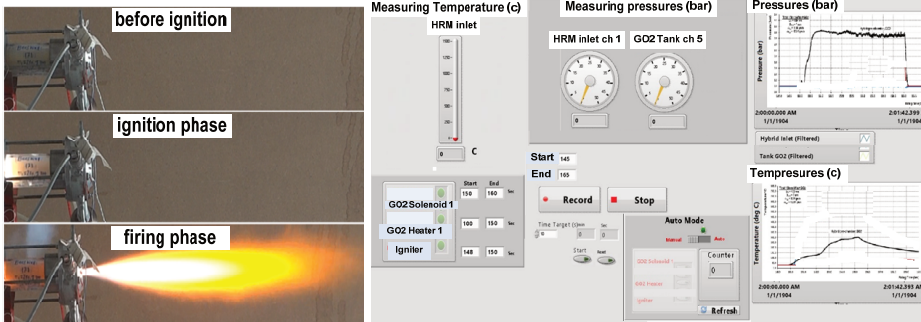*Fig. 3 Assembly drawing of the small scale HRM*

Fig. 4 Beeswax / gO₂ HRM firing test phases   Fig. 5 Lab-view software front panel

The 8.2 mm throat diameter graphite nozzle insert is designed to avoid degradation due to the excessive heat. gO$_2$ with the purity of $\approx$ 99.5 % is supplied via feed line which includes a high-pressure storage tank with a needle valve, a pressure regulator with safety valve, pressure gages, copper and Teflon pipe lines with Swagelok fittings connections, a solenoid valve, a heat exchanger with 500 W electric heater and a pressure transducer connector.

Fig. 5 is the front panel of Lab-view software and it is designed to issue the control commands through a 12 V DC signal that energizes switch relays to activate the igniter, heat exchanger and solenoid valve of gO$_2$ for a specified period. The recording system allows for the measurement of pressure and temperature profile in the HRM pre-chamber and gO$_2$ storage bottle, as shown in Fig. 6. The recording is started just before ignition system is triggered by 5.0 s and extended by 5.0 s after shut-off the firing. The tested HRM is operated fully automatically from the control room. The sequence of events is automatically controlled from a control panel of Lab-view software before the start of firing.

Pressure transducers are connected to measure the pressure at pre-chamber and gO$_2$ tank with a maximum value of 10 bar and 500 bar respectively. Temperature is measured in the pre-chamber by using a k-type thermocouple. The designed software programs using Lab-View and excel are employed to perform an analysis of the digitally measured data. Tab. 1 summarizes the experimental result data for beeswax / gO$_2$ HRM tests matrix.

Tab. 1 Experimental result data

| Test No.	m_{fu} (g)	$D_{fu,f\,avg}$ (mm)	dt_{ig} (s)	$dt_{SV\,GO2\,to\,open}$ (s)	$dt_{GO2\,SV\,to\,shutt}$ (s)	$t_{h,T}$ (s)	P_{TGO2} (bar)	$P_{h\,avg}$ (bar)	X_h (bar)	$T_{GO2,3}$ (oC)	$md_{fu\,av}$ (g/s)	$md_{GO2\,av}$ (g/s)	rd_{fu} (mm/s)	$G_{T\,avg}$ (g/mm²*s)	$(O/F)_h$ (-)	$C^*_{exp,h}$ (m/s)	$C^*_{th,h}$ (m/s)	Com. eff $^*_{exp,h}$ (%)
BW7-1	34.9	22.91	0.32	0.07	0.16	5.09	0.771	2.775	0.175	301.46	6.86	9.54	1.56	0.233	1.38	960.4	1755.0	54.7
BW7-2	36.7	23.29	0.29	0.10	0.14	5.10	0.852	2.784	0.228	293.76	7.19	10.46	1.60	0.250	1.45	950.9	1774.9	53.6
BW7-3	35.1	22.84	0.30	0.10	0.16	5.11	0.738	2.762	0.171	251.61	6.87	8.97	1.55	0.226	1.30	997.8	1768.9	56.4
BW7-4	32.0	21.94	0.28	0.10	0.15	5.12	0.737	2.888	0.139	291.66	6.25	9.06	1.46	0.220	1.44	1008.7	1775.3	56.8
BW7-5	32.0	21.81	0.32	0.15	0.16	5.09	0.769	3.012	0.126	234.72	6.29	9.45	1.46	0.226	1.50	1005.4	1779.4	56.5
BW7-6	33.0	22.01	0.30	0.15	0.16	5.11	0.703	3.151	0.150	317.56	6.46	8.55	1.47	0.215	1.33	1121.4	1860.3	60.3
BW7-7	38.6	Leakage failure test, bad assembly of solid fuel grain with front flange																

All firing tests have demonstrated an acceptable combustion stability as observed by the flame plume structure and acoustic characteristics for HRM. Tab. 1 summarizes the experimental results.
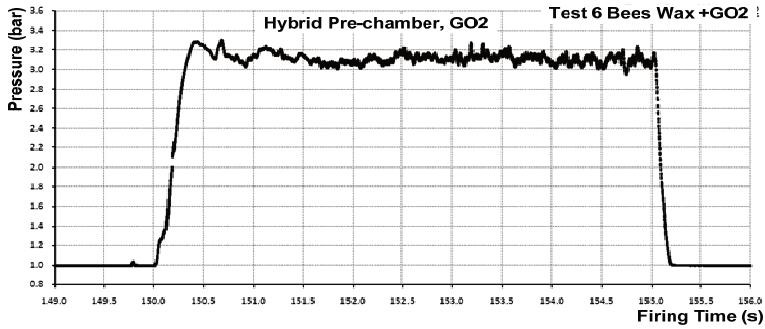
(a) Pre-chamber pressure
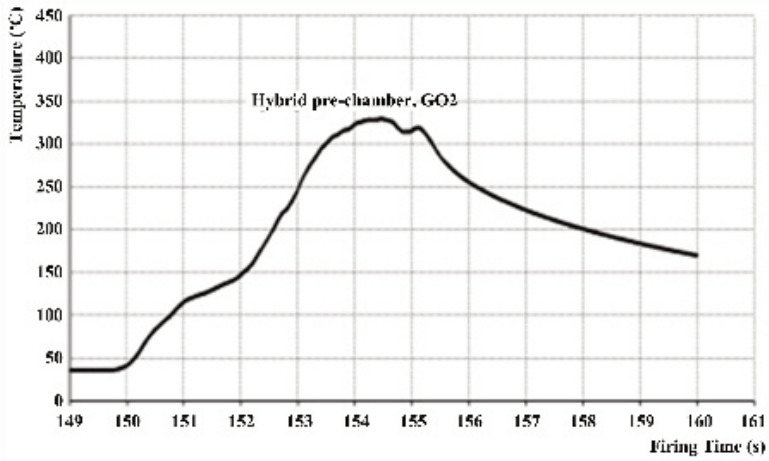
(b) Pre-chamber temperature
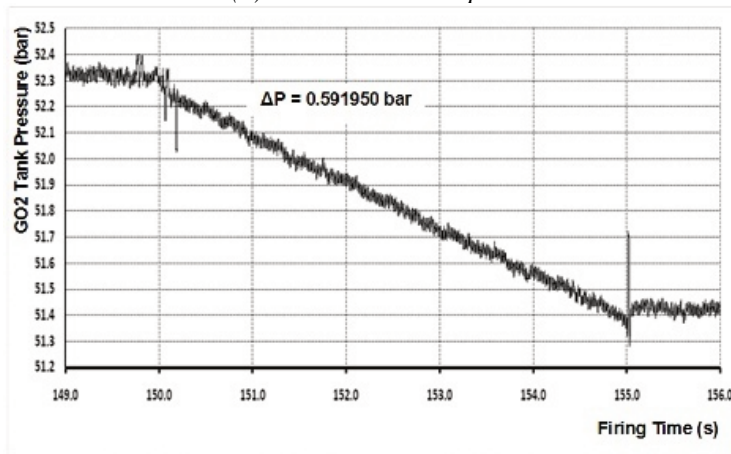
(c) gO₂ tank pressure

Fig. 6 HRM recording data during firing time

2.3. Beeswax Fuel Grain

Beeswax as solid fuel is selected for experimental work for several reasons as follows:
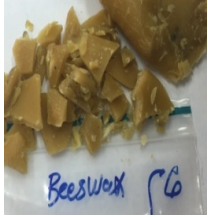- high performance regression rate similar to that of paraffin,
- environmentally safe as it is formed naturally by bees and produces a clean combustion exhaust gas,
- long storage without any change of physical and chemical properties,
- easily obtained from commercial companies (widely available),
- easily shaped into fuel grains and low cost.

Tab. 2 describes physical and thermodynamic properties of beeswax as solid fuel and oxygen gas as oxidizer.

The process of beeswax preparation starts by its heating using a controlled electric heater up to the temperature of ≈ 150 °C. This high temperature together with gentle stir leads to complete melting of solid beeswax. The molten beeswax is gradually poured into moulds and placed on a shaker about 10 minutes, to avoid possible creation of bubbles or cracks. The moulds are left at the ambient temperature for cooling. The excessive parts are trimmed and the grain cores are drilled at low speed.

The beeswax materials have a high tendency to shrink in volume during liquid-to-solid transformation; to avoid this, cast fuel grains are allowed to cool and re-solidify very slowly at room temperature. Thorough inspection showed the produced beeswax fuel grains free from bubbles or major cracks along the length.

Tab. 2 Physical and thermodynamic properties of beeswax and oxygen.

Symbol	Beeswax	Gas oxygen	
Chemical formula	$C_{46}H_{92}O_2$	O_2	
State at room temperature	Yellow, solid soft	Gas	
Class	Solid waxy	Gas oxidizer	
Molecular weight, [g/mol]	661.20	31.99	
Density, [kg/m³]	958.0-970.0	1.43	
Melting point, [°C]	62.0-64.0	−218.79	
Flammability point, [°C]	≈ 200.0	—	original role
Ignition point, [°C]	≥ 204.4	—	material
heat of formation, [kcal/mol]	−197.86	0.0	
(O/F)$_{sto.}$ with gO$_2$, [−]	3.32	—	
(O/F)$_{sto.}$ with air, [−]	14.10	—	

The final shapes of beeswax solid fuel grains have two configurations, full-scale and small-scale solid fuel grain, as shown in Fig. 7. The small-scale and full-scale castings can be burned for 5.0 s and 10.0 s respectively.

Fig. 8 shows the Xylon machine that produces the X-ray dose (V = 60 kV, I = 30 mA and duration 45 s). X-ray scan of the solid fuel grains checks for the availability of defects. Fig. 9 illustrates fuel grain ports (inlet and outlet), metal flanges (front and rear) for the full and small scales castings.

2.4. Ignition System

The most practical ignition method used for the firing tests is the NiCr ignition system, as NiCr coil charge igniter generates heat, fuel grain undergoes pyrolysis and the volatile products of pyrolysis burn with the injected oxidizer gO$_2$. The generated NiCr igniter flame reaches maximum intensity within a time delay of ≈ 0.25 s from ignition command, as shown in Fig. 10-a.

Full scale casting

-external grain diameter 50 mm,
-active port diameter 7 mm,
-grain length 100 mm,
-mould PMMA casing 3 mm
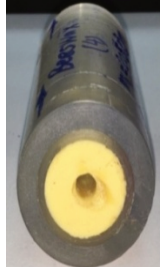
Small scale casting

-external grain diameter 50 mm,
-active port diameter 7 mm,
-grain length 100 mm,
-mould PMMA casing 3 mm thickness
 with inner diameter 35 mm
-PMMA casing 7.5 mm thickness

Fig. 7 Beeswax solid fuel grain after casting   *Fig. 8 Xylon machine*

Full grain   Front flange   Inlet port   Grain and remaining   Outlet port   Rear flange

Small grain   Front flange   Inlet port   Grain and remaining   Outlet port   Rear flange
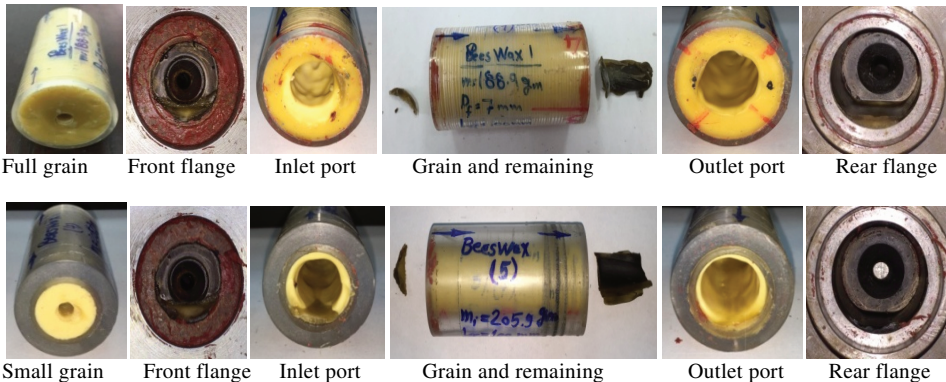
Fig. 9 Beeswax fuel grain and metal parts after firing

After inserting the NiCr igniter coil from the nozzle exit, a nozzle closure is glued to fix the ignition coil and to build up ignition pressure in order to reach a steady state combustion. The NiCr coil consists of a heat generator charge, connection wire, glue paper for fixation, control unit (DC 12 Volt relay switch), and A/C 200 V, 50 Hz power supply source. NiCr coil filament ignition system is shown in Fig. 10-a.

A longer ignition time delay is perceived if compared to the Pyrotechnical igniter (up to 0.8 s) [5]; mounting NiCr coil on the pre-chamber is a perfect location since the oxidizer gas flow over the fuel grain surface helps to achieve ignition easily along active channel grain, as shown in Fig. 10-b. The procedure to start ignition is described in Fig. 10-c.
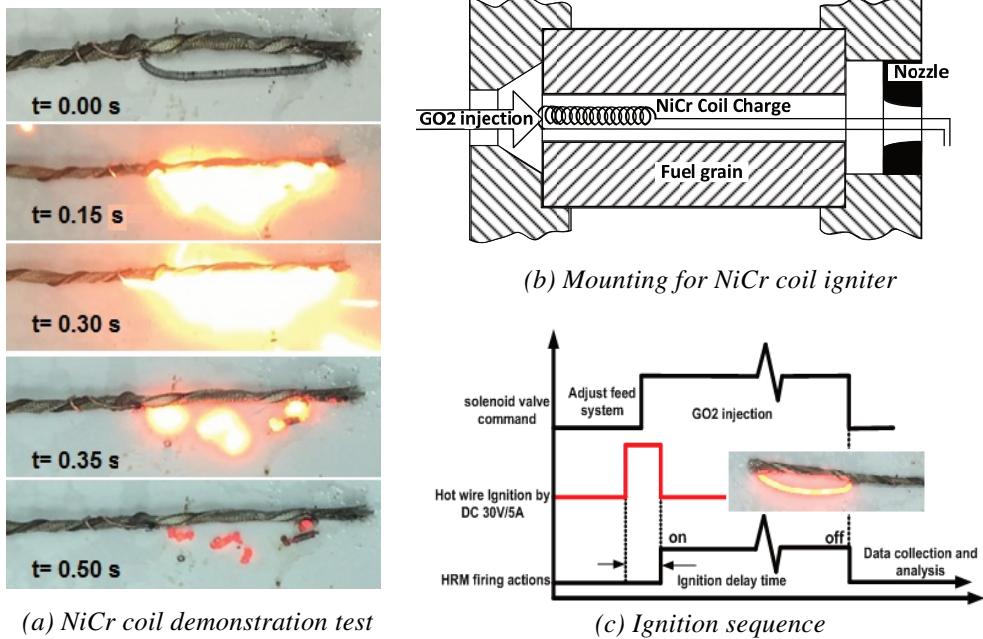
(a) NiCr coil demonstration test

(b) Mounting for NiCr coil igniter

(c) Ignition sequence

Fig. 10 NiCr ignition system

3. Failures During Firing

Throughout the development and testing of HRM, it is useful to depict some serious encountered problems which should be considered for any future work.

- Steel ally Nozzle burning during first design HRM firing, Fig. 11-a.
- Fuel grain seal failure, careful attention had to be paid during the process of assembly, Fig. 11-b.
- Igniter coil failure, the NiCr coil wire is broken due to bad manufacture or at some weak point created during coil winding, Fig. 11-c.
- Relay kit failure, caused by current overload or short circuit, Fig. 11-d.

4. Beeswax Combustion Process

Liquefied solid fuel combustion mechanism is proposed by Karabeyoglu and others [6, 7]; wax solid fuel regression rate is much faster than traditional solid fuels as PMMA, PE, since wax solid fuel burning surface has a higher melting layer, producing faster droplet entrainment process, as shown in Fig. 12.

Increasing the active channel length of the fuel grain leads to the increase of melting fuel accumulation and turbulence intensity. This increase is due to the increase in heat transfer surface area, which will cause a regression rate increase in the downstream direction. Beeswax regression rate calculation must include boundary layer blowing parameter (β), which is the ratio of flow thermal energy to gasification thermal energy of solid surface necessary to sustain the transformation solid to gas fuel.

(a) Steel ally nozzle burning during firing
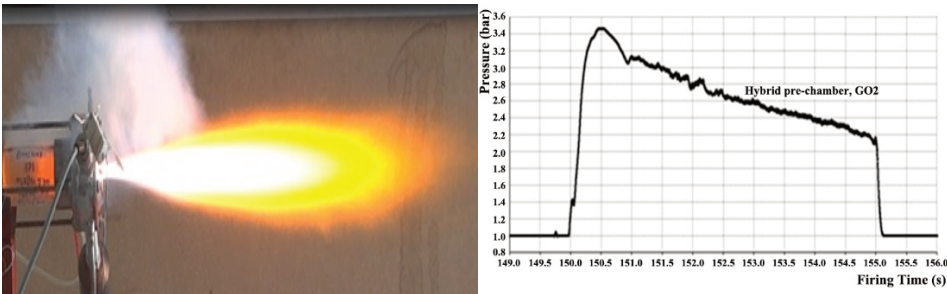
(b) Leakage phenomena during beeswax firing

(c) Igniter failure   *(d) Control kit (relay kit) failure*

Fig. 11 Typical failures encountered during beeswax firing
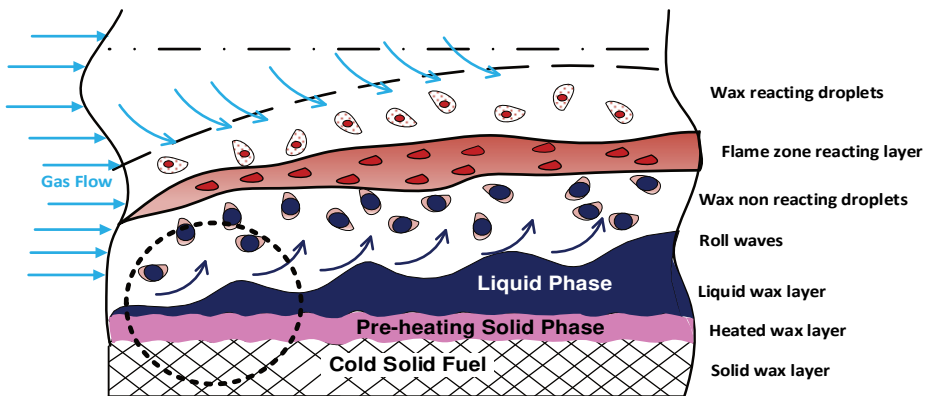

Fig. 12 Liquefying beeswax solid fuel combustion mechanism

The motivations for the observed behaviour of beeswax are due to the lower melting point effect, which causes fast changes in physical properties, such as viscosity μ and surface tension σ. The regression rate increases due to the increase of heat generation in the flame zone (by convection and radiation). The mentioned increase is due to the increase of the melting layer fuel gasification, low viscosity and surface tension. These parameters increase the regression rate of the new generation of solid fuel materials (beeswax and paraffin) over the traditional fuels (PMMA, PE).

Karabeyoglu's empirical formula to quantify the entrainment mass transfer for low melting point solid fuel is as follows [6],

$$\dot{M}_{ent} = function\left(\frac{(P_d)^\alpha h^\beta}{\sigma^\pi \mu^\gamma}\right), \tag{1}$$

where the upper part of the relation contains the operational parameters of the combustion (dynamic pressure P_d and (indirectly) the oxidizer mass flux, the lower part contains the fuel properties as surface tension σ and the melt layer viscosity μ. The exponents α and $\beta \approx$ 1-2 and γ and $\pi = 1$.

5. Results and Discussions

5.1. Regression Rate Formulation

In the region of small oxidizer mass flux ($G_{OX} < 10^{-4}$ g mm^{-2} s^{-1}), the regression rate of the solid fuel grain is influenced mainly by the heat transfer in the turbulent boundary layer while the combustion pressure, characteristic velocity or grain length has insignificant effect. Therefore, at the present conditions, the regression rate $\bar{r}_{fu}$ can be formulated as an empirical equation depending on oxidizer mass flux $\bar{G}_{ox}$ or total mass flux $\bar{G}_{tot}$ as,

$$\bar{r}_{fu(1)} = a\left(G_{ox}\right)^n. \tag{2}$$

If the total mass flux is considered, the formula of regression rate becomes as follows,

$$\bar{r}_{fu(2)} = a\left(G_{tot}\right)^n. \tag{3}$$

The parameters a and n are to be determined experimentally by measuring the regression rates at different values of oxidizer or total mass flux. The mass flux exponent n is of a main interest, because it has significant effect on the operating conditions.

Where the initial oxidizer and fuel mass fluxes, respectively as $\bar{G}_{ox,i} = \dfrac{\bar{m}_{ox}}{A_{fu,i}}$,

$\bar{G}_{fu,i} = \dfrac{\bar{m}_{fu}}{A_{fu,i}}$ the final oxidizer and fuel mass fluxes, respectively as $\bar{G}_{ox,f} = \dfrac{\bar{m}_{ox}}{A_{fu,f}}$,

$\bar{G}_{fu,f} = \dfrac{\bar{m}_{fu}}{A_{fu,f}}$ then the average oxidizer and fuel mass fluxes can be expressed as

$\bar{G}_{ox} = \dfrac{\bar{G}_{ox,i} + \bar{G}_{ox,f}}{2}$, $\bar{G}_{fu} = \dfrac{\bar{G}_{fu,i} + \bar{G}_{fu,f}}{2}$ and the average total mass flux G_{tot} is given by:

$$\bar{G}_{\text{tot}} = \dfrac{\dfrac{\bar{m}_{fu} + \bar{m}_{fox}}{A_{fu,i}} + \dfrac{\bar{m}_{fu} + \bar{m}_{ox}}{A_{fu,f}}}{2} \; . \tag{4}$$

Fig. 13 shows the burning rate versus mass flux for beeswax fuel. Beeswax regression rate reaches 1.58 mm s^{-1} at both oxidizers, and fuel mass flux reaches $0.133 \text{ g mm}^{-2} \text{s}^{-1}$ with gO_2, to establish average operating O/F about 1.40.

Fig. 13-a illustrates the beeswax regression rate coefficient $a \approx 3.070$ and $n \approx 0.352$ as function of oxidizer mass flux $G_{ox} \approx 0.133 \text{ g mm}^{-2} \text{s}^{-1}$ to produce average regression rate $\approx 1.509 \text{ mm s}^{-1}$. Fig. 13-b shows the effect of fuel mass flow rate (function of total mass flow rate G_{tot}) on beeswax regression rate at the same conditions, the regression rate coefficient increased to $a \approx 3.636$ and $n \approx 0.595$ as function of oxidizer mass flux $G_{ox} \approx 0.228 \text{ g mm}^{-2} \text{s}^{-1}$.
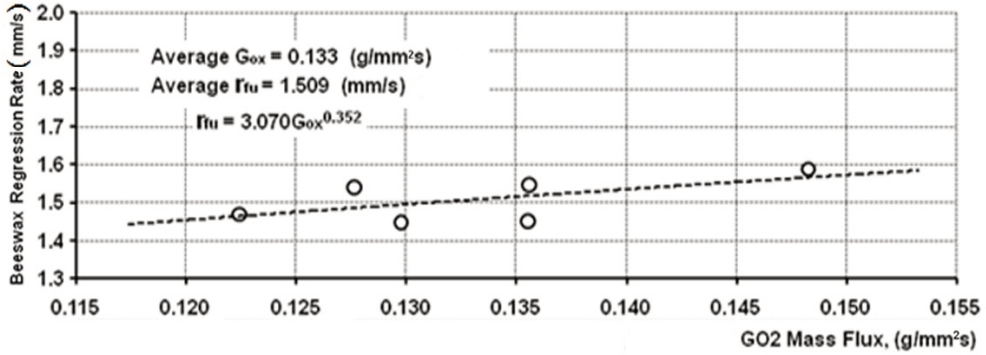
5.2. Regression Rate Evaluation

The average regression rate had been calculated $\bar{\dot{r}}_{fu,c}$ based on fuel grain mass loss as Eq. (5):

$$\bar{\dot{r}}_{fu,c} = \dfrac{\sqrt{\dfrac{4\left(m_{fu,i} - m_{fu,f}\right)}{\pi \rho_{fu} L_{fu}} + d_{po,i}^2} - d_{po,i}}{2 t_{bu}} \; . \tag{5}$$
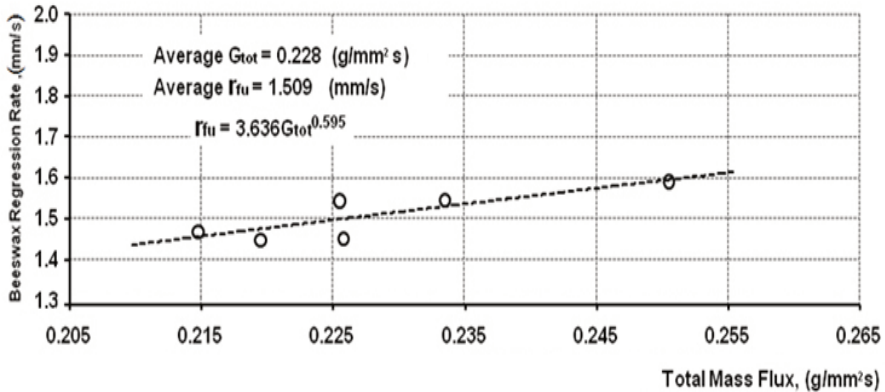
(a) Measured regression rate versus oxidizer mass flux

(b) Measured regression rate versus total mass flux

Fig. 13 Measured regression rate versus mass flux for beeswax fuel

The second method determines the average regression rate based on measuring $\bar{r}_{fu,m}$ the initial and final fuel grain port diameters $d_{po,i}$, $d_{po,f}$ and the burn time t_{bu} as

$$\bar{r}_{fu,m} = \frac{d_{po,f} - d_{po,i}}{2t_{bu}} \ , \tag{6}$$

where ρ_{fu} = solid fuel grain density, $m_{fu,I}$ = initial solid fuel grain mass, $m_{fu,f}$ = final solid fuel grain mass, and L_{fu} = fuel grain length. The comparison between measured and calculated average regression rate data indicates a maximum deviation less than 1.81 % for beeswax / gO_2 as shown in Fig. 14.
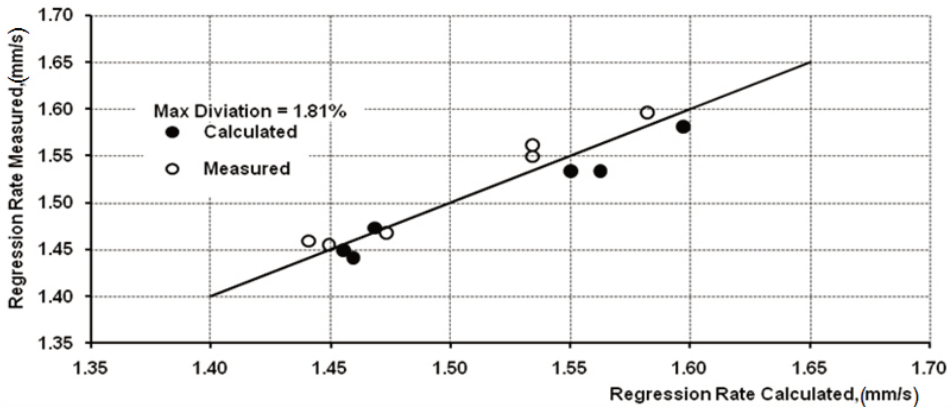

Fig. 14 Comparisons of beeswax average regression rate measured and calculated

5.3. Solid Fuel Mass Flow Rate

During engine firing run, the consumed beeswax solid fuel Δm_{fu} is measured and calculated $\bar{\dot{m}}_{fu,c}$ to evaluate further performance parameters. The average measured and calculated solid fuel mass flow rate $\bar{\dot{m}}_{fu,m}$, $\bar{\dot{m}}_{fu,c}$ is determined respectively as

$$\bar{\dot{m}}_{fu,m} = \frac{\Delta m_{fu}}{t_{bu}} = \frac{m_{fu,i} - m_{fu,f}}{t_{bu}}, \tag{7}$$

$$\bar{\dot{m}}_{fu,c} = \rho_{fu} A_{bu} \bar{\dot{r}}_{fu} = \rho_{fu} \pi \left(\frac{D_{fu,f} - D_{fu,i}}{2} \right) L_{fu} \left(\frac{\dot{r}_{fu,c} - \dot{r}_{fu,m}}{2} \right), \tag{8}$$

where Δm_{fu} is the solid fuel grain charge consumption, obtained by weighing the fuel grain before and after the test, A_{bu} = solid fuel grain burning surface. Fig. 15 shows the comparison between measured and calculated average solid fuel mass flow rate data, which indicates a maximum deviation less than 0.96 %.
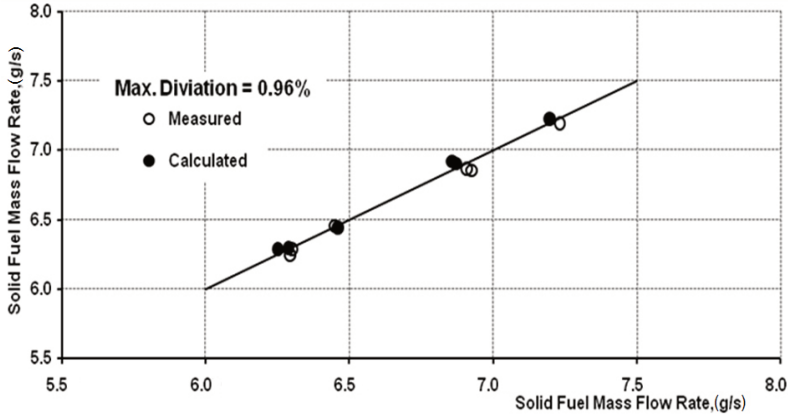

Fig. 15 Comparisons of beeswax average mass flow rate measured and calculated

5.4. Combustion Efficiency Computation

The experimental characteristic velocity c_{exp}^* is calculated as:

$$c_{exp}^* = \frac{\bar{p}_{av} A_{th}}{\bar{\dot{m}}_{h,t}}. \tag{9}$$

The average theoretical characteristic velocity c_{th}^* can be determined by thermo-chemistry code [8] as follows

$$c_{th}^* = \frac{\sqrt{RT_c}}{\Gamma}. \tag{10}$$

where $\Gamma = \sqrt{\gamma} \left(\frac{2}{\gamma+1} \right)^{\frac{\gamma+1}{\gamma(\gamma-1)}}$ and γ = the ratio of specific heats of combustion products, R = the gas constant, T_c = the combustion chamber gas temperature. The combustion efficiency of combustion chamber η_c could be calculated by comparing theoretical and experimental values of the characteristic velocity as:

$$\eta_c = \frac{c_{exp}^*}{c_{th}^*}, \quad [\%]. \tag{11}$$

The average consumed gO_2 mass flow rate $\bar{\bar{m}}_{ox}$ as oxidizer and beeswax solid fuel mass flow rate $\bar{\bar{m}}_{fu}$ during HRM firing, the corresponding mixture ratio O/F is obtained as

$$\left(\frac{O}{F}\right)_h = \frac{\bar{\bar{m}}_{ox}}{\bar{\bar{m}}_{fu}} .$$
(12)

Fig. 4 demonstrates incomplete combustion process inside HRM which produces high length of flame exhaust with different ranges of colour: (white, yellow and orange). Fig. 15 illustrates poor combustion efficiency for beeswax / gO_2 HRM. Fig. 16 illustrates the operating average O/F for HRM $\approx$ 1.4 (fuel rich) to establish average combustion characteristic velocity (combustion efficiency = $C*$ ratio) $\approx$ 56.4 % since the calculated $(O/F)_{sto}$ for beeswax / gO_2 combustion is 3.32.

6. Conclusion

The above study shows an advantage of using the new generation of waxy hydrocarbon fuels over the classical polymeric fuels (PMMA, PE), as they illustrate about triple times higher regression rate at similar operating conditions.

Over 7 firing test runs using beeswax / gO_2 are performed at variations of oxidizer mass flow rate ($\approx$ 8.55 – 10.46 $g\,s^{-1}$) and a constant initial active port of 7 mm diameter, the consumed solid fuel mass in these tests during 5 s firing is $\approx$ 32.0 – 36.7 g.

The beeswax as solid fuel is extremely safe and with higher regression rate during HRM firing, that is associated with higher mass flow rate of gases generated from burning surface and the subsequent combustion of fuel-rich products.
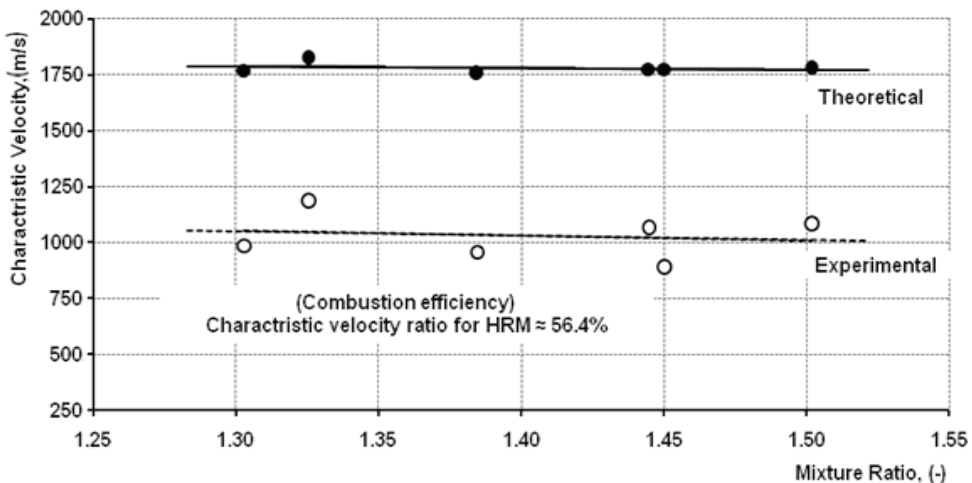

Fig. 16 Comparisons beeswax / gO_2 characteristic velocity measured and calculated

Beeswax regression rate reaches 1.58 $mm\,s^{-1}$ at a fuel mass flux of 0.133 $g\,mm^{-2}\,s^{-1}$, and establishes an average operating O/F about 1.40.

The NiCr ignition system showed a longer time delay of ≈ 0.25 s, which is a low performance parameter.

References

[1] SUTTON, G.P. *Rocket Propulsion Elements: An Introduction to the Engineering of Rocket*. New York: Wiley, 1992. 656 p. ISBN 978-0-471-52938-5.

[2] MAKLED A.EL-S. and AL-TAMIMI, M.K. Hybrid Rocket Motor Performance Parameters: Theoretical and Experimental Evaluation. *International Journal of Aerospace and Mechanical Engineering,* 2017, vol. 11, no. 1, p. 47-55. ISSN 2393-8609.

[3] KRISHNAN, S. Hybrid rocket technology: An overview. In *Proceedings of the 6th Asia Pacific International Symposium on Combustion and Energy Utilization.* Kualalumpur: Faculty of Mechanical Engineering, Universiti Teknologi Malaysia Malaysia, 2002, 602 p. ISBN 978-9-835-20244-5.

[4] ALTMAN, D. Hybrid Rocket Development History. In *27th Joint Propulsion Conference,* Sacramento, 1991, p. 1-5. DOI 10.2514/6.1991-2515.

[5] MAKLED A.EL-S. and AL-TAMIMI, M.K. Experimental Investigation of Hybrid Rocket Motor: Ignition, Throttling and Re-Ignition Phenomena. *International Journal of Aerospace and Mechanical Engineering*, 2017, vol. 11, no. 11, p. 2086-2096. ISSN 2393-8609.

[6] KARABEYOGLU, M.A. and CANTWELL, B.J. Combustion of Liquefying Hybrid Propellants: Part 1. *Journal of Propulsion and Power*, 2002, vol. 18, no. 3, p. 610-620. DOI 10.2514/2.5975.

[7] KARABEYOGLU, M.A. and CANTWELL, B.J. Combustion of Liquefying Hybrid Propellants: Part 2, *Journal of Propulsion and Power*, 2002, vol. 18, no. 3, p. 621–630. DOI 10.2514/2.5976.

[8] GORDON, S and McBRIDE, B.J. *Computer Program for Calculation of Complex Chemical Equilibrium Composition and Application. NASA Reference Publication 1311*. [Research Report]. [on-line]. 1994. [cited 2018-05-12]. Available from: https://www.grc.nasa.gov/www/CEAWeb/RP-1311.pdf.